Role of the Cosurfactant in the CTAB/Water/*n*-Pentanol/*n*-Hexane Water-in-Oil Microemulsion. 1. Pentanol Effect on the Microstructure†

Gerardo Palazzo,*,‡,§ Francesco Lopez,‡ Mauro Giustini,‡,|| Giuseppe Colafemmina,‡,§ and Andrea Ceglie‡

Consorzio Interuniversitario per lo sviluppo dei Sistemi a Grande Interfase (CSGI), c/o Department of Food Technology, University of Molise, I-86100 Campobasso, Italy, Department of Chemistry, University of Bari, I-70126, Bari, Italy, and Department of Chemistry, University "La Sapienza", I-00185 Roma, Italy

Received: July 2, 2002; In Final Form: November 27, 2002

The microstructure of the quaternary water-in-oil microemulsion CTAB/water/*n*-pentanol/*n*-hexane has been investigated by means of the pulsed gradient spin−echo NMR technique over a wide range of composition. The composition of the continuous organic phase and of the interfacial phase has been determined through the analysis of the *n*-pentanol self-diffusion coefficient. The size of the reverse aggregates has been evaluated from the CTAB self-diffusion coefficient. The correlation of the reverse micellar size with interfacial composition has therefore been possible. Results coming from both water dilution lines and interface dilution lines have been analyzed according to suitable models. A "master plot", i.e., a graphical representation that allows us to display the data collected at all the possible compositions of the four components system, is also proposed.

1. Introduction

The term microemulsion,[1] in its most general use, denotes a thermodynamical stable, oil/water mixture, stabilized by (at least) a third component able to reduce the oil−water interfacial tension (surfactant). Characteristic lengths are of the order of tens of nanometers, so that microemulsions appear optically transparent (some times bluish) and isotropic. Since their discovery, microemulsions have been subject to numerous theoretical and experimental investigations. On the applied front, they are of interest in enhanced oil recovery, cutting oils, pharmaceutics, cosmetics, detergency, lubrication, etc. From the fundamental research perspective, microemulsions are interesting because their structure can be idealized as a set of interfaces, so that they represent archetypal *complex fluids*. Over the past three decades, it has been shown that microemulsions are structurally well-defined self-organized systems that can assume a wide variety of microstructures. These comprise phases consisting of droplets of water-in-oil (w/o microemulsions or L_2 phases), or droplets of oil-in-water (o/w microemulsions or L_1 phases), as well as bicontinuous phases. The structural evolution of microemulsions upon changing parameters such as temperature, salinity of aqueous phase, and so on has been rationalized.[2,3] Good agreement between theory and experiments has been found in the case of ternary microemulsions[4] (where the surfactant resides exclusively at the interface). However, to attain the appropriate packing of amphiphiles at the interface, the addition of other surface-active substances is often required. These cosurfactants (usually medium chain linear alcohol) partition themselves among the oil, water, and interface domains. Therefore, without a quantitative description of the dependence of the partition equilibria on the system composition, a full understanding of quaternary microemulsions cannot be attained.

In this paper we determine the interfacial composition of CTAB/water/*n*-pentanol/*n*-hexane microemulsions over a wide range of composition. Then the size of the w/o droplets is discussed in terms of water content and surface composition.

2. Materials and Methods

2.1. Microemulsion. All the chemicals were purchased from Sigma. Hexadecyltrimethylammonium bromide (CTAB) was three times recrystallized from anhydrous ethanol, and stored over dried silica gel under vacuum. *n*-Hexane (UV spectroscopy grade) and *n*-pentanol, POH (ACS grade), have been used without any further purification.

Three parameters are needed to define the composition of a four-component system in a single-phase region. In this paper we will use the water/CTAB (W_0) and the *n*-pentanol/CTAB (P_0) mole ratios, the third parameter being either the *n*-hexane/CTAB (N_0) mole ratio or the *overall* surfactant concentration, [CTAB].

The microemulsions were prepared by weighing the appropriate amounts of surfactant, alcohol, *n*-hexane, and water needed to obtain the desired P_0, N_0, and $W_0 = 5$ (for $W_0 < 5$ the microemulsion does not exist). Microemulsions at different W_0 values were prepared by water dilution of the microemulsion at $W_0 = 5$.

For the calculations the following molar volumes have been used:[5,6] CTAB = 0.3609 L/mol; H_2O = 0.01853 L/mol; *n*-pentanol = 0.10824 L/mol; the molecular volume of the trimethylammonium bromide moiety of CTAB (v_{HG}) was assumed equal to 141 Å^3;[5] the tail length of CTAB and *n*-pentanol were assumed to be 21.7 and 7 Å, respectively (calculated according to Tanford[7]).

† Paper prepared to mark the 60th birthday of Björn Lindman, honoring his contribution to the fundamentals and applications of surfactant self-assembly.

* Corresponding author. Address: Dipartimento di Chimica, via Orabona 4, I-70126, Bari, Italy. E-mail: palazzo@chimica.uniba.it.

‡ CSGI-University of Molise.

§ University of Bari.

|| University "La Sapienza".

10.1021/jp026430o CCC: $25.00
Published on Web 01/30/2003

TABLE 1: CTAB and *n*-Pentanol Self-Diffusion Coefficients and the Corresponding Partition Constant *R*

system composition			experimental data[a]		evaluated data (see text for details)				
W_0	[CTAB] (mol L^{-1})	P_0	$10^9 D_{CTAB}$ (m^2 s^{-1})	$10^9 D_{POH}$ (m^2 s^{-1})	$10^2 P_{mic}$	$10^3 \phi^{bulk}$	$10^3 \phi^{int}$	η^b (mPa s)	R[c]
6.9	0.060	8.2	0.204	1.52	30 ± 3	955 ± 4	38 ± 2	0.310	11 ± 2
6.9	0.060	10	0.242	1.48	32 ± 3	950 ± 2	43 ± 2	0.313	10 ± 2
6.9	0.060	12	0.277	1.40	36 ± 4	942 ± 3	50 ± 3	0.317	11 ± 2
6.9	0.060	14	0.277	1.37	37 ± 4	937 ± 4	56 ± 4	0.320	10 ± 2
6.9	0.060	16	0.300	1.31	40 ± 4	929 ± 4	64 ± 4	0.323	10 ± 2
6.9	0.060	18	0.328	1.29	41 ± 5	923 ± 5	67 ± 6	0.328	9 ± 2
6.9	0.060	20	0.323	1.23	44 ± 5	913 ± 6	80 ± 7	0.330	9 ± 2
36.0	0.095	7.9	0.062	1.19	36 ± 4	875 ± 3	64 ± 3	0.320	8 ± 2
45.0	0.093	12	0.073	1.03	50 ± 5	830 ± 7	94 ± 6	0.326	9 ± 3
5.0	0.100	14	0.310	0.82	63 ± 7	860 ± 10	130 ± 10	0.322	11 ± 4
5.0	0.100	20	0.530	0.65	63 ± 7	820 ± 15	170 ± 15	0.341	8 ± 3
8.3	0.085	6.1	0.140	1.22	41 ± 4	937 ± 3	51 ± 2	0.307	12 ± 3
8.4	0.081	6.4	0.140	1.48	32 ± 3	940 ± 2	49 ± 2	0.307	9 ± 2

[a] Uncertainty on diffusion coefficients is 4%. [b] Viscosity of the continuous phase; uncertainty = 2%. [c] Partition constant (molar standard state) evaluated according to eq 2.

2.2. Viscosity Measurements. Both the viscosity and density measurements of *n*-hexane/*n*-pentanol solutions were performed at 298 ± 0.01 K by means of an automatic viscosity system (AVS/G and AVS/S) manufactured by SCHOOT (accuracy better then 1%).

2.3. PGSE-NMR. Self-diffusion coefficient measurements have been carried out by the Fourier transform NMR pulsed field gradient spin−echo (PGSE-NMR) method.[8] Experiments were performed on a BS-587A NMR spectrometer (Tesla), operating at 80 MHz for protons, equipped with a pulsed field gradient unit (Autodif 504, STELAR s.n.c). The pulse sequence employed was the Stejskal−Tanner[9] sequence, 90°−τ−180°−τ−echo, with two rectangular field gradient pulses of about 0.04 T m^{-1} and duration δ, separated by a constant interval Δ. The echo amplitude recorded at 2τ is given by

$$A(2\tau) = \exp[-2\Delta/T_2] \exp[-\gamma^2 G^2 \delta^2 (\Delta - \delta/3) D]$$

where T_2 is the spin−spin relaxation time, γ is the proton gyromagnetic ratio, and D is the self-diffusion coefficient of the species responsible of the spin−echo decay. The strength of the applied field gradient (G) was determined before each experiment by a separate calibration with pure DMSO. The value of the DMSO self-diffusion coefficient was from the literature.[10] The magnetic field was locked by an external D_2O lock signal for all the samples. The temperature of the samples was maintained at 298.0 ± 0.2 K by means of a built-in variable temperature control unit. The accuracy of the self-diffusion coefficients was within 4%.

3. Results and Discussion

3.1. *n*-Pentanol Partitioning between Dispersed and Continuous Phases. We have previously demonstrated that, for [CTAB] ∼ 0.1 M and P_0 ∼ 8, the L_2 region of the CTAB/water/*n*-pentanol/*n*-hexane microemulsion is constituted of water droplets stabilized by a surfactant/cosurfactant interfacial film.[11,12] The surfactant, CTAB, is soluble only to a minute amount in *n*-hexane/*n*-pentanol; a higher solubility requires about five molecules of water per surfactant molecule.[11,12]

This scenario holds also for the wider composition range explored in the present work. Indeed, the self-diffusion coefficient of *n*-hexane[13] is around 3×10^{-9} m^2 s^{-1} (not shown), well above the diffusion coefficients of water[14] and CTAB (see Table 1). Otherwise, the cosurfactant diffusion is consistent with its partition between the dispersed and the continuous phases (see below). The determination of the composition of the dispersed and continuous phase is central to understanding the microstructure of the system.

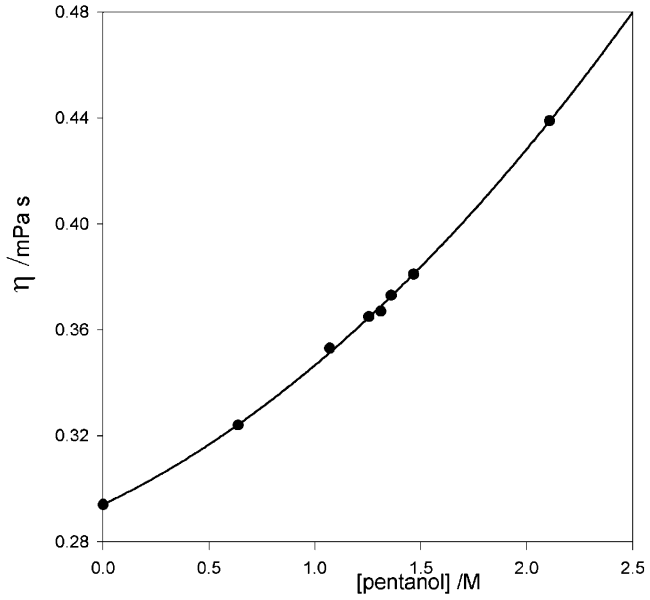

Figure 1. Viscosity of binary mixtures *n*-pentanol/*n*-hexane. The curve is a second-order best-fit polynomial.

The alcohol concentration could have a 2-fold influence on the diffusion of the aggregates. The variation in the continuous phase composition surely induces changes in the viscosity of the medium surrounding the particles. Indeed, the viscosity of *n*-pentanol/*n*-hexane binary mixtures is heavily dependent on the *n*-pentanol concentration as shown in Figure 1. Moreover, the modification of the interfacial composition could drive variations in both the structure and the dimensions of the aggregates. To discriminate between these two effects, it is necessary to determine the amount of *n*-pentanol present in both the dispersed and the continuous phase.

Such a determination can be done through the comparison of the measured self-diffusion coefficient of *n*-pentanol (in principle, also SANS measurements can furnish the interface composition; see for example ref 15). Generally, the exchange of materials (surfactant, water and cosurfactant molecules) between the aggregates and the continuous phase is fast on the time scale of a PGSE experiment (10^{-1} s). Under this condition, the observed self-diffusion coefficient of a given compound is the weight average of self-diffusion coefficients in the two sites: the micelle (D^{mic}) and the continuous bulk (D^{bulk}) according to Lindman's law:[16]

$$D^{obs} = P_{mic}D^{mic} + (1 - P_{mic})D^{bulk} \quad (1)$$

where P_{mic} is the fraction of molecules moving with the micelles. The self-diffusion coefficient of the micelle can be assumed to be equal to the self-diffusion coefficient of a compound present only on the micelle. In the system under investigation, the best candidate is the CTAB due to its poor solubility in *n*-hexane/*n*-pentanol mixtures. Indeed, comparison between DLS and PGSE data confirmed that $D_{CTAB} \equiv D^{mic}$.[11] D^{bulk} is the self-diffusion coefficient of the compound moving in a continuous bulk phase. In the case of *n*-pentanol, the choice of the true value of D^{bulk} is difficult, because the amount of *n*-pentanol in a mixture with *n*-hexane strongly affects its viscosity (see Figure 1) and, as a consequence, its self-diffusion coefficient, as well as those of all the other diffusing species. To overcome this problem, an iterative procedure was used. In the first step, all the alcohol was assumed to be present in the bulk phase, and (from the data of Figure 1) a first value of the bulk phase viscosity, $\eta(1)$, was therefore evaluated. Assuming that for the *n*-pentanol $D^{bulk}\eta$ = constant = 6.4×10^{-13} N (the error, 2%, in this equality is less than experimental uncertainty) the first value for the self-diffusion coefficient of the *n*-pentanol diffusing in the bulk, $D^{bulk}(1)$ was calculated. Using $D^{bulk}(1)$, eq 1 allows us to obtain the first value of the fraction of *n*-pentanol in the micelle, $P_{mic}(1)$. From $P_{mic}(1)$ one can easily determine a second composition of the bulk phase, and the corresponding viscosity, $\eta(2)$, which allows the evaluation of $D^{bulk}(2)$ and therefore of $P_{mic}(2)$, and so on. Within four to five iterations, the above-described procedure converges. Table 1 lists the self-diffusion coefficient of CTAB and *n*-pentanol measured at different W_0 and P_0 values together with the corresponding fraction of micellar *n*-pentanol. Equation 1 does not allow us to discriminate if the alcohol is partitioned preferentially in the water or in the interfacial film. However, the low *n*-pentanol solubility in water[17] and the high tendency of *n*-pentanol to partition into direct micelles[18] strongly suggests that in the reverse micelles *n*-pentanol is solubilized essentially in the interfacial film. Both the oil and interfacial phase volume fractions (ϕ^{bulk} and ϕ^{int}, respectively) can then be calculated (see Table 1). Assuming ideal behavior (activity coefficients = 1), the partition constant for the *n*-pentanol between the interfacial and the oil phase can be evaluated as

$$R = \frac{[POH]^{int}}{[POH]^{bulk}} = \frac{P_{mic}}{1 - P_{mic}} \frac{\phi^{bulk}}{\phi^{int}} \quad (2)$$

The *n*-pentanol concentrations in both interface and continuous phase, determined from PGSE experiments, are presented in Figure 2.

The data (listed in Table 1) are consistent with a constant value of $R = 10$ and do not show any dependence on the W_0 parameter (in agreement with the assumption of a negligible solubility of *n*-pentanol on the water pool). For comparison, the results obtained by means of cosurfactant titration are shown in the same figure. This is effected by adding oil at constant water and surfactant level to destabilize an otherwise stable w/o microemulsion and restabilizing it by the addition of a requisite amount of cosurfactant.[19] The data so collected were used to construct graphs (such as the one shown in the inset of Figure 2) by plotting the mole ratio alcohol/surfactant (P_0) vs the mole ratio oil/surfactant (N_0). The striking linearity of such plots is consistent with the assumption that the composition of both dispersed and continuous phases are constant through the dilution/titration procedure.[19] Therefore the intercept corresponds

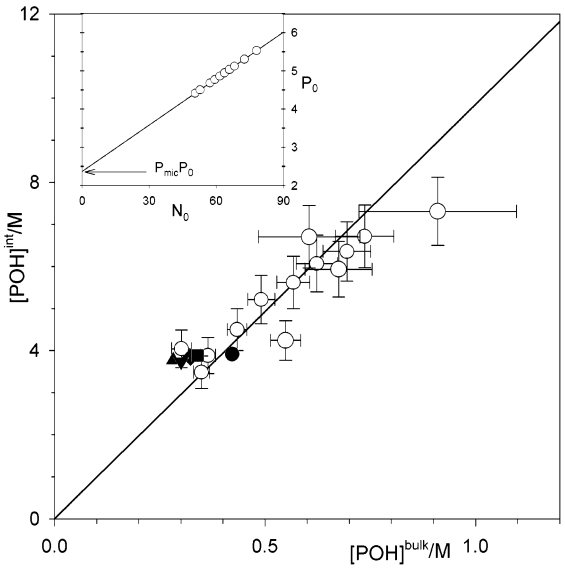

Figure 2. Correlation between *n*-pentanol concentrations in the continuous phase and in the interface. Empty circles represent data coming from PGSE-NMR. The concentrations were evaluated according to eq 2 using the data of Table 1; note that the uncertainty on P_{mic} is reflected on both axes. Also shown is the prediction of eq 2 for $R = 10$ (straight line). Filled symbols represent results obtained by means of cosurfactant titration of the interface: (▲) $W_0 = 40$; (▼) $W_0 = 21$; (◆) $W_0 = 8$; (■) $W_0 = 15$; (●) $W_0 = 60$. Inset: a representative titration plot ($W_0 = 8$). The intercept on the ordinate axis gives the alcohol/CTAB mole ratio at the interface (P_0P_{mic}).

to the (constant) mole ratio *n*-pentanol/CTAB in the dispersed phase ($P_{mic}P_0$ in our notation), and the slope is the (constant) mole ratio *n*-pentanol/*n*-hexane in the continuous bulk. These values have been used to evaluate the corresponding composition of the interfacial and continuous phases. As shown in Figure 2 the results obtained by titration are consistent with those from PGSE data. In particular, the partition constant obtained by titration ($R \sim 12$) agrees within experimental error with the average R obtained from Table 1 ($\langle R \rangle = 10 \pm 2$).

Overall the data support a model where the cosurfactant partitions itself between the continuous and interfacial phases according to eq 2.

There are two implications. First, the system microstructure will depend on W_0, P_0 and, also, on the overall surfactant concentration. Second, once R has been determined, we can evaluate P_{mic} and, therefore, the composition of the interfacial film and of the continuous phase simply from the stoichiometric composition of the system, as described in the Appendix. This is an important point, because, due to an unlucky combination of short T_2 relaxation time, and *J*-coupling, a safe determination of the self-diffusion coefficient of *n*-pentanol via PGSE-NMR is often a difficult task to effort in the system under investigation.[11]

3.2. Reverse Micelles Size: Water Dilution Lines. The insight gained so far on the composition of interfacial and bulk phases allows us to tackle the task of micellar size.

For spherical particles at infinite dilution the self-diffusion coefficient (D°) is related to the particle hydrodynamic radius (R_h) via the Stokes−Einstein equation

$$D^\circ = \frac{K_B T}{6\pi\eta R_h} \quad (3)$$

where K_B is the Boltzman constant and T is the absolute temperature. For an ensemble of particles at *finite* concentration,

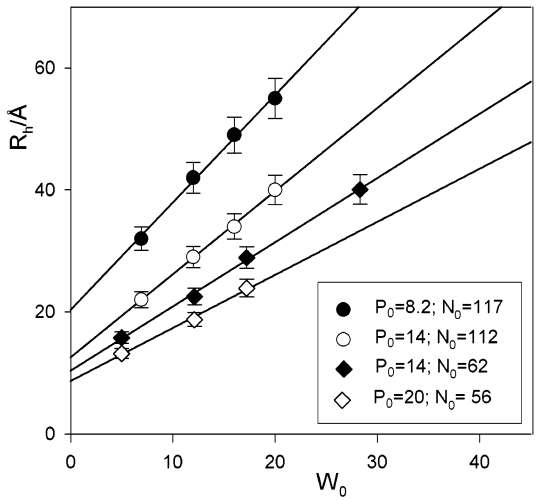

Figure 3. Hydrodynamic radii as a function of W_0 along water dilution lines. Straight lines are the best fits according to eq 5.

the measured self-diffusion (D_{mic}) is related to $D°$ of eq 3 through a virial expansion whose first term is[20]

$$D_{mic} = D°(1 - k\phi_{mic}) \tag{4}$$

where ϕ_{mic} is the droplet volume fraction (the sum of water and interfacial volume fraction in the present case) and k is a constant that depends on the interparticles interactions. Previous investigations indicate that for the CTAB/water/pentanol/hexane microemulsion the k value is 2[11,12] (corresponding to hard spheres with only hard-core interactions).[20,21] A knowledge of the bulk phase composition and, therefore, of its viscosity, η, permits the determination of the hydrodynamic radius of reverse micelles via eqs 3 and 4.

As long as the *n*-pentanol partition is unaffected by the W_0 parameter, the analysis of reverse micelles size along water dilution lines is trivial.

For a given headgroup area of the surfactant (a_S), the total interfacial surface is $n_S a_S = n_{mic} 4\pi R_w^2$ (where R_w is the water core radius and n_{mic} and n_S are the number of micelles, and surfactant, respectively). The volume of the aqueous phase composed of water and surfactant headgroup, is $n_S v_{HG} + n_W v_W = n_{mic} 4\pi R_w^3/3$ (where v_{HG} is the headgroup volume and v_W is the water molecular volume). The ratio between the volume of the aqueous phase and the interfacial area gives $R_w = 3(v_{HG} + v_W W_0)/a_S$. From diffusion experiments, one obtains the hydrodynamic radius R_h

$$R_h = L_{int} + \frac{3v_{HG}}{a_S} + \frac{3v_W W_0}{a_S} = L + \frac{3v_W W_0}{a_S} \tag{5}$$

where L_{int} is the thickness of the interfacial layer. For a_S constant, the equation predicts a linear relation between R_h and W_0. For data collected along water dilution paths, a plot of R_h versus W_0 should then result in a straight line whose slope and intercept are $3v_W W_0/a_S$ and $L_{int} + 3v_{HG}/a_S$, respectively. We remark in passing that some authors[22] neglect the term $3v_{HG}/a_S$, so that the intercept corresponds to the interfacial film thickness, L_{int}. In the absence of cosurfactant, this last term can be assumed equal to the length of the surfactant tail. But in the present case the film is composed of surfactant and cosurfactant and consequently the situation is more complicated (see below). Plots of R_h vs W_0 are presented in Figure 3 for some water dilution lines. In these experiments water is added to a stock solution at $W_0 = 5$ or 7, giving a family of samples in which

TABLE 2: Results of Analysis of Water Dilution Paths

P_0	N_0	L/Å	a_s/Å^2	a^*/Å^2	P_0P_{mic}	X_{POH}
6	68	22 ± 3	41 ± 4	21 ± 1	2.3 ± .3	0.70 ± 0.02
7.9	67	16 ± 2	60 ± 1	16 ± 1	2.8 ± 0.3	0.74 ± 0.02
8.2	117	20 ± 1	51 ± 1	15 ± 1	2.4 ± 0.3	0.71 ± 0.02
8.7	66	18 ± 1	72 ± 4	14 ± 1	4.0 ± 0.3	0.80 ± 0.02
10	64	15.4 ± 0.5	70 ± 1	17 ± 1	3.1 ± 3	0.76 ± 0.02
12	63.4	17.5 ± 0.5	99 ± 2	13 ± 1	7.0 ± 0.7	0.87 ± 0.01
14	112.2	12.5 ± 0.5	66 ± 1	11 ± 1	5.0 ± 0.6	0.83 ± 0.01
14	61.6	10 ± 0.5	86 ± 3	9 ± 1	9 ± 1	0.90 ± 0.01
18	109	10 ± 2	70 ± 10	8 ± 1	7.4 ± 0.8	0.88 ± 0.02
20	56.4	9.7 ± 0.6	120 ± 9	9 ± 1	13 ± 1	0.93 ± 0.01

[CTAB] varies (due to water dilution) but the mole ratio oil/CTAB = N_0 remains constant. This is the rationale for the choice of this last parameter to characterize the system, along with P_0 and W_0. Figure 3 reveals two interesting features: a striking linearity of the plots, and the different trends for two curves sharing the same *overall* ratio POH/CTAB ($P_0 = 14$) but different N_0 values. This last feature clearly depends on the partition of *n*-pentanol so that, due to different ϕ_{bulk} and ϕ_{int} values, the two lines have different values of interfacial composition (see Table 2). The former feature confirms the validity of eq 5. Accordingly, the values of a_S and L have been evaluated for all the water dilution lines and are listed in Table 2. An inspection of Table 2, reveals that an increase in the amount of *n*-pentanol at the interface induces an increase in the mean area per CTAB molecule coupled with a decrease in the L value.

By comparing the values of a_S and L obtained at different interfacial composition, is possible to understand their dependence on the relative amount of alcohol and surfactant in the interface. Let us discuss the mean area per surfactant molecule first. The experimental evidence is that a_S increases with the number of alcohol molecules present at the interface. This implies that upon addition of cosurfactant molecules at the interface, the total interfacial surface increases (in agreement with studies on DDAB-based w/o microemulsions).[23] The simplest model describing this process supposes additive contribution of alcohol and surfactant to the total interfacial area

$$\text{total surface} = n_{CTAB} a°_{CTAB} + n_{POH} a°_{POH} \tag{6}$$

where $a°_{CTAB}$ ($a°_{POH}$) is the contribution of a CTAB (*n*-pentanol) molecule to the interfacial area. The interfacial film composition can be expressed as the mole fraction (at the interface) of *n*-pentanol, X_{POH}. It is useful to define a mean area, a^*, averaged over the amphiphiles (CTAB *plus n*-pentanol) at the interface

$$a^* = \frac{\text{total surface}}{n_{CTAB} + n_{POH}} = (1 - X_{POH}) a_S$$
$$= a°_{CTAB} - X_{POH}(a°_{CTAB} - a°_{POH}) \tag{7}$$

In Figure 4 a^* values are reported as function of X_{POH} for all the available data. The linear regression, according to eq 7 is also shown. The extrapolated value at $X_{POH} = 1$ gives the alcohol contribution to the interfacial surface. The value, $a°_{POH} = 7 \pm 2$ Å, is smaller than the cross-sectional area of densely packed hydrocarbon chains (~20 Å) and close to the effective area of a hydroxyl group (8 Å).[24] The extrapolation at $X_{POH} = 0$ gives the polar head area in the hypothetical reverse micelle stabilized only by CTAB molecules. The value, $a°_{CTAB} = 36 \pm 10$ Å^2, has a large uncertainty (because of the lack of data for $X_{POH} < 0.7$) but compares satisfactorily with the CTAB headgroup area estimated in reverse micelles prepared without cosurfactant

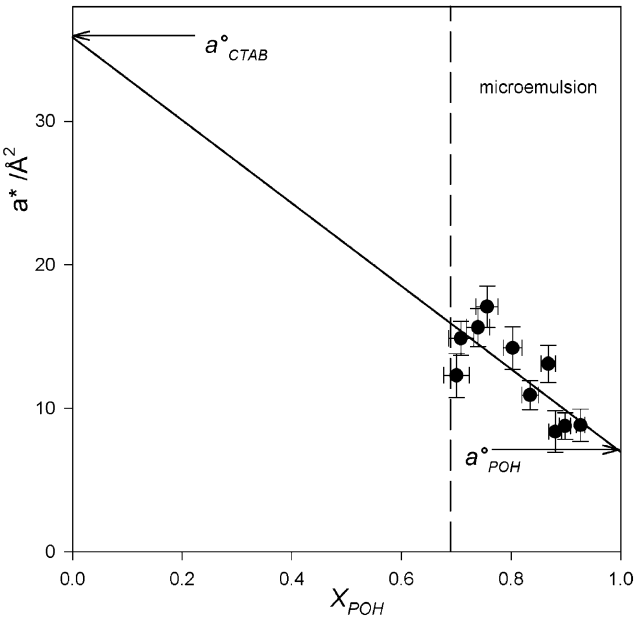

Figure 4. Mean area per amphiphile (eq 7) as a function of interface composition. The abscissa represents the mole fraction of pentanol at the interface $X_{POH} = P_0P_{mic}(1 + P_0P_{mic})^{-1}$. Note that the one-phase microemulsion exists only for $X_{POH} > 0.7$. Points are the data of Table 2, straight line represent the best-fit according to eq 7, the extrapolations at $X_{POH} = 0$ and $X_{POH} = 1$ are also indicated.

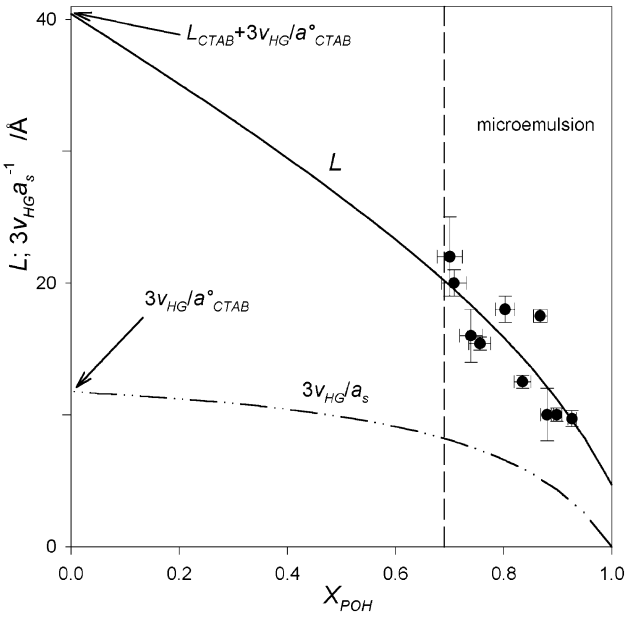

Figure 5. L against X_{POH}. L is the intercept of the R_h vs W_0 plot (as those shown in Figure 3). Points come from Table 2. The nonlinear least-squares fit according to eqs 5, 7, and 8 is shown as a continuous curve. Also shown is the behavior of the term $3v_{HG}/a_S$ (dashed−dotted curve). The extrapolation of both the curves at $X_{POH} = 0$ is indicated (note the lack of data for $X_{POH} < 0.7$ where the microemulsion does not exist).

(solvent isooctane-chloroform)[25] and at the air/water interface[26] (45 and 43 Å^2, respectively).

Once the dependence of a_S on X_{POH} is assessed, an analysis of the influence of this parameter on L (the intercept of the R_h vs W_0 plots) can be made. First, $L = L_{int} + 3v_{HG}a_S^{-1}$ (eq 5) so that an increase in a_S will result in a decrease of L. However, such an effect can account for less than half of the decrease found experimentally on *n*-pentanol addition shown in Figure 5. This evidence indicates that the "effective film thickness" is also a function of the film composition. The thickness, L_{int}, "seen" in a PGSE experiment is strictly a hydrodynamic quantity (deduced from measurements of hydrodynamic radii). The rationalization for this behavior on the basis of molecular properties is difficult to obtain. Two limits can be identified: (i) In the hypothetical case of an interface without cosurfactant, the film thickness should depend only on some surfactant molecular parameter. (ii) At the other extreme, in reverse micelles stabilized only by an alcohol film, the thickness of such an hypothetical film will only depend on the properties of *n*-pentanol molecules. Between these two limits, i.e., in the realm of "real" film composition, we assume a thickness for the interfacial layer as a composition average of the thickness of pure CTAB (L_{CTAB}) and *n*-pentanol (L_{POH}) films:

$$L_{int} = (1 - X_{POH})L_{CTAB} + X_{POH}L_{POH} \qquad (8)$$

The L values of Table 2 have been fitted (see Figure 5) to the equation $L = L_{int} + 3v_{HG}a_S^{-1}$, with L_{int} given by eq 8, and a_S depends on the interface composition according to eq 7 (with $a^\circ_{CTAB} = 36$ Å^2 and $a^\circ_{POH} = 7$ Å^2). The best-fit values, $L_{CTAB} = 28 \pm 8$ Å and $L_{POH} = 5 \pm 2$ Å, compare favorably with the lengths of aliphatic moieties (21.7 and 7 Å, respectively).

3.3. Reverse Micelles Size: Interface Dilution Paths. Table 1 indicates that an enrichment of the interface in *n*-pentanol (increase in P_0P_{mic}) will result in a decrease in the reverse micellar size (increase in D_{CTAB}). This is qualitatively in agreement with the results obtained in the previous section.

To describe quantitatively the effect of the interface composition on micellar size, it is better to develop a new analysis of the data obtained from variations in ratio of POH/CTAB/oil at constant W_0 value. This is so for two reasons. First, the simple model outlined in the previous section is fairly crude (although successfully encapsulating most of the phenomena). The best fit parameters, a_S and L, exhibit large uncertainties; therefore they should be determined independently. This can be done directly by observing the dependence of the hydrodynamic radius on interface composition. A second reason is a practical one. We are interested in studying the dependence of microstructure on the interfacial composition. This is because this parameter seems to play a pivotal role in the activity of enzymes[27] and on the structure of DNA[28] when they are solubilized in reverse micelles. In this case, an experimental approach based on water dilution lines would require a huge number of samples (for each P_0 value a whole family of samples varying in the W_0 would be required). Further, the errors in the a_S and L values obtained could obscure subtle changes in the microstructure.

Hence an analysis tailored for sets of samples at constant W_0 and different P_0P_{mic} values would be advantageous.

The starting point is eq 5 that through eqs 7 and 8 can be rewritten as

$$R_h = L_{CTAB} - X_{POH}(L_{CTAB} - L_{POH}) + (1 - X_{POH})\frac{3(v_{HG} + v_W W_0)}{a^\circ_{CTAB} - X_{POH}(a^\circ_{CTAB} - a^\circ_{POH})} \qquad (9)$$

whence eq 9 becomes

$$R_h = R_h^\circ - X_{POH}\left[(L_{CTAB} - L_{POH}) + \frac{3(v_{HG} + v_W W_0)}{a^\circ_{CTAB}}\frac{1}{y - X_{POH}(y - 1)}\right] \qquad (10)$$

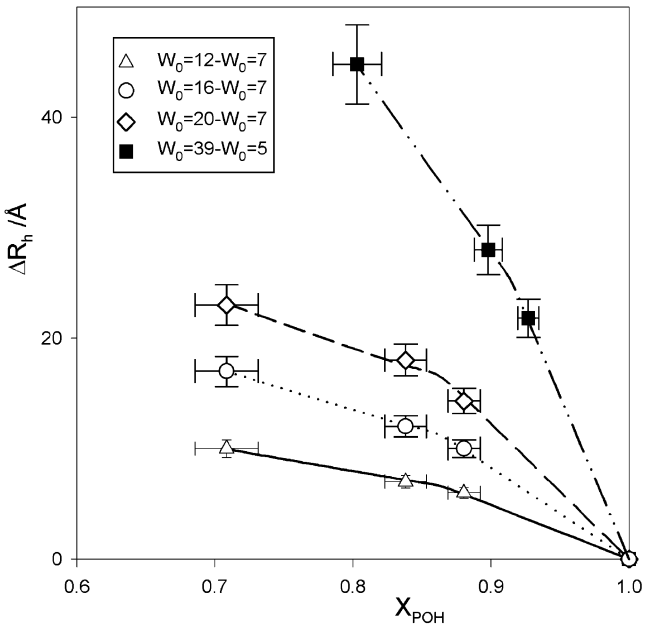

Figure 6. Difference in hydrodynamic radii between microemulsion droplets at $W_0 = 12$ (△), $W_0 = 16$ (○), $W_0 = 20$ (◇), and $W_0 = 39$ (■) and a reference microemulsion at the same interface composition (X_{POH}) and different W_0. The W_0 value of the reference was 7 for empty symbols and 5 for filled squares. Lines are nonlinear least-squares fits to eq 11.

where $R_h^\circ = L_{CTAB} + 3(\upsilon_{HG} + \upsilon_W W_0)/a_{CTAB}^\circ$ is the hydrodynamic radius of the hypothetical reverse micelle made of only CTAB ($P_0 = 0$) and $y = a_{CTAB}^\circ/a_{POH}^\circ$. Equation 10 contains four free parameters (R_h°, ($L_{CTAB} - L_{POH}$), y, a_{CTAB}°) and is highly nonlinear, so that any attempt to fit the experimental data to it is useless. The number of fitting parameters can be reduced if we focus our attention on the difference in the hydrodynamic radii between microemulsions differing *only* in their W_0 values.

$$\Delta R_h = R_h(W_0 2) - R_h(W_0 1) = \frac{3\upsilon_W(W_0 2 - W_0 1)}{a_{CTAB}^\circ} \frac{y(1 - X_{POH})}{y(1 - X_{POH}) + X_{POH}} \quad (11)$$

As expected, in eq 11 the dependence on the interface thickness disappears, and ΔR_h will depend only on the difference in water content and on the contribution of surfactant and cosurfactant to the interfacial area. Equation 11 can be applied to subsets of data having the same interfacial composition (X_{POH}) and two different W_0 values. Experimentally, they were prepared as *n*-pentanol dilution lines of samples at different W_0 values. The utmost care must be paid to have exactly the *same* CTAB/*n*-pentanol/*n*-hexane ratios for samples at different W_0's (to have the *same* X_{POH} values). Several ΔR_h were evaluated by subtracting (for each X_{POH} value) the hydrodynamic radius obtained at a W_0 value taken as (arbitrary) reference from the R_h obtained at other W_0. The curves ΔR_h vs W_0 have been subsequently fitted to eq 11. The results, shown in Figure 6, are characterized by an excellent agreement between experimental points and the fits. Further, from these best-fit parameters, essentially the same values were obtained for a_{CTAB}° and a_{POH}° (33 ± 3 and 7 ± 1 Å^2, respectively) found in the analysis of water dilution lines in the previous section. Once a_{CTAB}° and a_{POH}° have been so determined, the remaining free parameters in eq 10 are R_h° and ($L_{CTAB} - L_{POH}$). The analysis of the water dilution lines strongly suggest that L_{CTAB} and L_{POH} can be identified with the tail lengths of surfactant and cosurfactant, so that ($L_{CTAB} - L_{POH}$) can be safely assumed equal to 14 Å. In Figure 7A are reported the hydrodynamic radii plotted against X_{POH} for samples at different W_0 values. Each subset at fixed W_0 was fitted to eq 10 using R_h° as the only adjustable parameter (the lines in Figure 7 are the nonlinear least-squares fits).

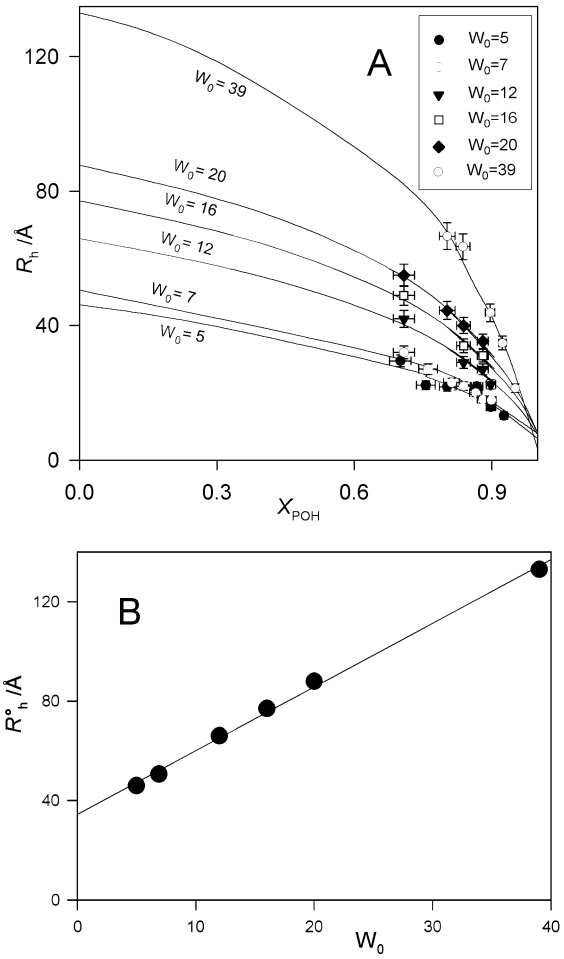

Figure 7. Effect of interfacial composition on reverse micelle size. Panel A: Influence of X_{POH} on the hydrodynamic radii for samples at fixed W_0 (reported in the legend). Points are experimental data; curves indicate the nonlinear least-squares fits according to eq 10. Note that the extrapolation at $X_{POH} = 0$ (i.e., R_h°) depends on the W_0 value; such a dependence is illustrated in panel B.

For each W_0, one R_h° value was obtained, and such values when plotted vs the water content lead to the graph presented in Figure 7B. These R_h° values represent the hydrodynamic radii of hypothetical reverse micelles formed in the absence of any cosurfactant at all. Therefore, in Figure 7B is presented another water dilution line and the data, according to eq 5, lay on a straight line. The intercept, $L_{CTAB} + 3\upsilon_{HG}/a_{CTAB}^\circ$, is 34 ± 1 Å and corresponds to $L_{CTAB} \equiv 22$ Å in excellent agreement with the length of CTAB tail (21.7 Å) and with estimate of the previous section. From the values $L_{CTAB} = 22$ Å and the assumed value of $L_{CTAB} - L_{POH} = 14$ Å, one obtains $L_{POH} =$ 8 Å. Again, the agreement with the result independently obtained from the analysis of water dilution paths is striking.

To conclude this section, it is worth mentioning that the data can be directly fitted to eq 10, leaving both R_h° and $L_{CTAB} - L_{POH}$ as free parameters. The fits obtained in this case are indistinguishable from those of Figure 7A (one free parameter), but with very large associated errors (>60%). This is probably due to the strong nonlinearity of eq 10.

3.4. Putting It All Together: A Master Plot. In the two previous sections it has been demonstrated how the data obtained

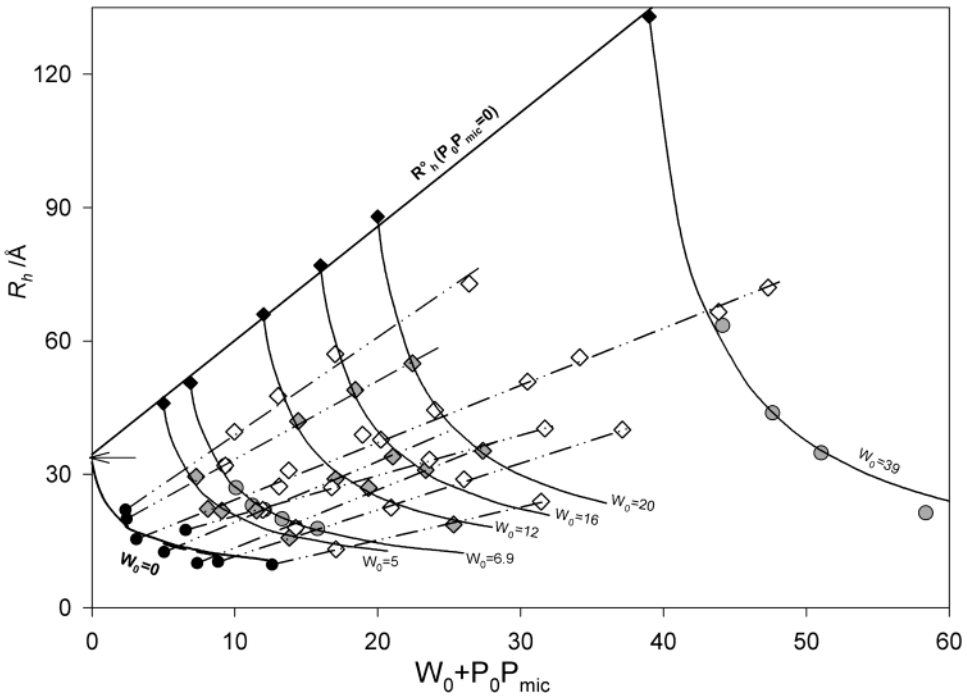

Figure 8. Master plot (see text for details). Hydrodynamic radius as a function of the sum of the mole ratios water/CTAB and POH/CTAB (this last evaluated at the interface; see paragraph 3.1). Straight dot−dashed lines indicate water dilution lines (at constant P_0P_{mic} values listed in Table 2), and diamonds denote the data fitted according to eq 5. Thin continuous curves indicate interface dilution lines (at constant W_0 values, indicated in the graph), and gray symbols denote the data fitted according to eq 10. In some cases the same points were used in both fits (gray diamonds). Extrapolated data are denoted by black symbols. The extrapolation at zero cosurfactant content of interface dilution lines (black diamonds) represents a water dilution line of reverse micelles without cosurfactant (R_h° bold straight line). The intercepts of water dilution lines (black circles) represent an interface dilution path of dry reverse micelles ($W_0 = 0$ bold curve). The arrow denotes the radius of dry reverse micelles without cosurfactant ($L_{CTAB} + 3\upsilon_{HG}/a^\circ_{CTAB}$) and coincides with the extrapolation at abscissa = 0 of both the R_h° and $W_0 = 0$ paths.

along water and cosurfactant dilution paths can be analysed separately. To evaluate the mutual consistency of these two approaches it is useful to represent the two sets of data (and the relative analysis) on the same graph. This allows insight into the overall composition−microstructure relationship.

According to eq 9, the size of the reverse micelles depends on only two parameters, viz. W_0 and the interfacial composition (related to the overall composition through eq A3 of the Appendix). The strategy applied in this work has been to plot R_h against W_0 *plus* P_0P_{mic}. We chose P_0P_{mic} as the term that accounts for the interfacial composition because it shares the same order of magnitude of W_0, so that the influence of both water and alcohol content are equally weighted in the plot. In such a "master plot", the data fall into place on patterns such as those illustrated in Figure 8. According to eq 5, straight lines (dot−dashed) may easily be drawn through points sharing the same P_0P_{mic}, so allowing the extrapolation to $W_0 = 0$. There is an evident analogy between this "master plot" and the Zimm plot used in light scattering.[29] However, by contrast with the Zimm plot, the influence of the second parameter (the interfacial composition in the present case) on R_h cannot be linearized. Therefore through the points sharing the same W_0, we draw on eq 10 (rewritten in terms of P_0P_{mic}) to extrapolate to zero *n*-pentanol content. The R_h values extrapolated at $P_0P_{mic} = 0$ (black squares of Figure 8) coincide with the R_h° of Figure 7B. These R_h° values represent a family of points at constant (null) alcohol content, which allow the extrapolation of R_h° to $W_0 = 0$ (bold straight line). The linear regression of the data at constant P_0P_{mic} gives, as intercepts at $W_0 = 0$, a set of data at constant (null) water content (black diamonds). Further, these points follow eq 10 and can be extrapolated numerically to $P_0P_{mic} = 0$ (bold curve). Inspection of Figure 8 reveals that the same state of *dry* reverse micelles made of *only* CTAB molecules (with $R_h = L_{CTAB} + 3\upsilon_{HG}/a^\circ_{CTAB}$ indicated by the arrow in Figure 8) can be reached in two independent ways: by reducing to zero the water content of hypothetical micelles depleted in *n*-pentanol (the R_h° straight line), or with vanishing *n*-pentanol content of dry micelles (the $W_0 = 0$ curve). Remarkably, the two extrapolations lead to the same numerical value (33 ± 1 Å). It should be stressed that the line at $P_0P_{mic} = 0$ and the curve at $W_0 = 0$ do not correspond to real systems. In fact, one requires a minimum of about 2.4 *n*-pentanol molecules *per* CTAB molecule in the interface,[11,12] and of at least 5 water molecules *per* CTAB molecule[11,12] to have a one-phase microemulsion. However, the real and the hypothetical (extrapolated data) microemulsions behave in the same way, following the prediction of eq 9. This is a strong indication that the reverse micelles remain spherical upon water and alcohol addition, without any change in shape or connectivity. The analysis of the master plot of Figure 8 reveals that the effects of *n*-pentanol and water on the microstructure are essentially uncoupled. Indeed, cosurfactant and water act independently as local and global geometric packing constraints (respectively) of the interface geometry.

Local packing of cosurfactant and surfactant sets the spontaneous curvature of interface, its flexibility and therefore the *preferred* size of noninteracting aggregates. Water acts as a global constraint (conservation of volume fractions). These two constraints alone are sufficient to determine the size of the aggregates in a wide range of compositions.[2]

4. Conclusions

PGSE-NMR experiments reveal that *n*-pentanol partitions strongly into the interfacial film. The dependence of the interface composition on the overall composition is described satisfac-

torily by a simple partition equilibrium. This permits a quantitative analysis of the experimental data directly in terms of interface composition. To achieve this result, a new strategy has been developed for two composition paths: (i) water dilution lines, where the interface composition remains constant; (ii) paths where the interface composition is changed at fixed W_0 (due to the partition equilibrium, such paths correspond either to cosurfactant dilution either to oil dilution). All the data recorded along different paths can be analysed by the same "master plot" and reveal the following features:

Adding water to the CTAB/water/*n*-pentanol/*n*-hexane microemulsion always results in an increment of the reverse micellar radii. Such an increment is tuned by the total interfacial area, which is fixed by the amount of cosurfactant in the film. The loading of *n*-pentanol into the interface corresponds to the *increase* in the total interface with a corresponding *decrease* of the interfacial film thickness. Such an arrangement of the film contributes to the preservation of the negative interfacial curvature. Only (spherical) inverse structures, without any transition to bicontinuous structure were found.

Acknowledgment. We thank Prof. Barry Ninham for the critical reading of the manuscript.This work was supported by the MIUR of Italy (PRIN 2001 STRUTTURA E DINAMICA DI SISTEMI A GRANDE INTERFASE) and by the Consorzio Interuniversitario per lo sviluppo dei Sistemi a Grande Interfase (CSGI-Firenze).

Appendix

The evaluation of the fraction of *n*-pentanol present at the interface, through eq 2, is complicated by the fact that both the volume fraction of the interfacial phase, ϕ^{int}, and the volume fraction of the continuous bulk phase, ϕ^{bulk}, depend on P_{mic}.

Actually, if we indicate with V_{CTAB}, V_{POH}, V_w, and V_o the molar volume of CTAB, *n*-pentanol, water, and oil, respectively, and with N_o the molar ratio *n*-hexane /CTAB we have

$$\phi^{bulk} = \frac{N_o V_o + (1 - P_{mic}) P_0 V_{POH}}{V_{CTAB} + W_0 V_w + N_o V_o + P_0 V_{POH}}$$

$$\phi^{int} = \frac{V_{CTAB} + P_{mic} P_0 V_{POH}}{V_{CTAB} + W_0 V_w + N_o V_o + P_0 V_{POH}} \qquad \text{(A1)}$$

Equation 2 can be rewritten as

$$P_{mic} = \frac{R}{R + \frac{\phi^{bulk}}{\phi^{int}}} \qquad \text{(A2)}$$

Inserting eq A1 into A2 and solving for P_{mic}, one finds

$$P_{mic}^{\,2}[P_0 V_{POH}(R-1)] + [N_o V_o + P_0 V_{POH} + R(V_{CTAB} - P_0 V_{POH})] - R V_{CTAB} = 0 \qquad \text{(A3)}$$

note that N_o is related to the overall surfactant concentration through

$$[CTAB]^{-1} = V_{CTAB} + P_0 V_{POH} + W_0 V_w + N_o V_o$$

Therefore, P_0, W_0, and N_o are known from the system's overall composition. If also R is known (as in the present case), eq A3 can be solved analytically to give the unknown P_{mic}.

References and Notes

(1) For reviews see: De Gennes, P. G.; Taupin, C. *J. Phys. Chem.* **1982**, *86*, 2294. Langevin, D. *Acc. Chem. Res*. **1988**, *21*, 255. Gelbart, W. M.; Ben-Shail, A. *J. Phys. Chem.* **1996**, *100*, 13169.

(2) Hyde, S. T.; Andersson, S.; Larsson, K.; Blum, Z.; Landh, T.; Lidin, S.; Ninham, B. W. In *The Language of Shape*; Elsevier: Amsterdam; 1997; p 170.

(3) Safran, S. A. In *Statistical Thermodynamics of Surfaces, Interfaces, and Membranes*; Addison-Wesley Publishing Co.; New York, 1994; p 247.

(4) Hyde, S. T.; Ninham, B. W., Zemb, T. *J. Phys. Chem*. **1989**, *93*, 1464. André, P.; Ninham, B. W.; Pileni, M. P. *New J. Chem*. **2001**, *25*, 563.

(5) Reiss-Husson, F.; Luzzati, V. *J. Phys. Chem.* **1964**, *68*, 3504.

(6) *Handbook of Chemistry and Physics*, 65th ed.; CRC Press Inc.: Boca Raton, FL, 1984−1985.

(7) Tanford, C. *J. Phys. Chem.* **1972**, *21*, 3020.

(8) Stilbs, P. *Prog. NMR Spectrosc*. **1987**, *19*, 1.

(9) Tanner, J. E.; Stejskal E. O. *J. Chem. Phys*. **1968**, *49*, 1768.

(10) Holz, M.; Mao, X.; Seiferling, D.; Sacco, A. *J. Chem. Phys*. **1996**, *104*, 669.

(11) Giustini, M.; Palazzo, G.; Colafemmina, G.; Della Manica, M.; Giomini, M.; Ceglie, A. *J. Phys. Chem*. **1996**, *100*, 3190.

(12) Colafemmina, G.; Palazzo, G.; Balestrieri, E.; Giomini, M.; Giustini, M.; Ceglie, A. *Prog. Colloid Polym. Sci*. **1997**, *105*, 281.

(13) Hexane self-diffusion coefficients were evaluated from the slope of the echo decay of $-CH_2-$ at short δ values and from the $-CD_2-$ and $-CD_3$ decays in samples doped with C_6D_{14}.

(14) The water self-diffusion coefficients are slightly higher than those of CTAB because of water partition between the reverse micelles and organic bulk (see ref 11). Because the water dissolved in the bulk is well below 10% of total water amount, we neglect this feature in the present treatment.

(15) Bumajdad, A.; Eastoe, J.; Griffiths, P.; Steytler, D. C.; Heenan, R. K.; Lu, J. R.; Timmins, P. *Langmuir* **1999**, *15*, 5271.

(16) Nilsson, P. G.; Lindman, B. *J. Phys. Chem*. **1983**, *87*, 4756. Nilsson, P. G.; Lindman, B. *J. Phys. Chem*. **1984**, *88*, 5391.

(17) Aveyard, R.; Mitchell, R. W. *J. Chem. Soc., Faraday Trans. 1* **1969**, *65*, 2645.

(18) The partition constant for the process POH(water) → POH(direct micelles) is ∼36 for DTAB; see: Inglese, A.; De Lisi, R.; Milioto, S. *J. Phys. Chem.* **1996**, *100*, 2260.

(19) Bowcott, J. E.; Schulman, J. H. *Z. Elektrochem*. **1955**, *59*, 283. Birdi, K. S. *Colloid Polym. Sci*. **1982**, *26*, 628. Moulik, S. P.; Digout, L. G.; Aylward, W. M., Palepu, R. *Langmuir* **2000**, *16*, 3101.

(20) Ohtsuki, T.; Okano, K. *J. Chem. Phys*. **1982**, *77*, 1443.

(21) Lekkerkerker, H. N. W.; Dhont, J. K. G. *J. Chem. Phys*. **1984**, *80*, 5790.

(22) See for example Luisi, P. L.; Giomini, M.; Pileni, M. P.; Robinson, B. H. *Biochim. Biophys. Acta* **1988**, *947*, 209.

(23) Maidment, L. J.; Chen, V.; Warr, G. G. *Colloids Surf. A* **1997**, *129−130*, 311.

(24) Rao, I. V.; Ruckenstein, E. *J. Colloid Interface Sci.* **1986**, *113*, 375.

(25) Lang, J.; Mascolo, G.; Zana, R.; Luisi, P. L. *J. Phys. Chem*. **1990**, *94*, 3069.

(26) Lu, J. R.; Hromadova, M.; Simister, E. A.; Thomas, R. K.; Penfold, J. *J. Phys. Chem*. **1994**, *98*, 11519.

(27) Lopez, F.; Cinelli, G.; Ambrosone, L.; Colafemmina, G.; Ceglie, A.; Palazzo, G. Submitted.

(28) Airoldi, M.; Boicelli, C. A.; Gennaro, G.; Giomini, M.; Giuliani, A. M.; Giustini, M.; Scibetta, L. *Phys. Chem. Chem. Phys.* **2002**, *4*, 3859.

(29) Zimm, B. H. *J. Chem. Phys.* **1948**, *16*, 1099.